Spin correlations and short-range magnetic order in the honeycomb layered $Na_2Ni_2TeO_6$

Artem Korshunov, Irina Safiulina, Alexander Kurbakov**

A. N. Korshunov, Prof. A. I. Kurbakov
NRC «Kurchatov Institute» - PNPI, Orlova roshcha 1, Gatchina, 188300, Russia
Saint Petersburg University, Universitetskaya nab. 7-9, Saint Petersburg, 198504, Russia
E-mail: artem.korshunov91@gmail.com, kurbakov_ai@pnpi.nrcki.ru

I. A. Safiulina
Institut Laue-Langevin, Avenue de Martyrs 71, Grenoble, 38042, France
École polytechnique fédérale de Lausanne, Laboratory for Quantum Magnetism, Lausanne, CH-1015, Switzerland

Keywords: magnetism, honeycomb structure, neutron scattering, diffuse magnetic scattering

An experimental study of long-range magnetic order formation mechanisms in a layered structure with a honeycomb arrangement of the magnetic atoms $Na_2Ni_2TeO_6$ has been carried out. For the first time, the strong spin correlations were directly observed above the Neel temperature T_N that was manifested in the presence of broad diffuse peaks on neutron diffraction patterns obtained with XYZ polarization analysis. Due to the possibility of separating the magnetic, nuclear incoherent and nuclear coherent contributions to the total neutron scattering cross section, it was unequivocally established that observed diffuse scattering has magnetic nature. The spin pair correlation function was reconstructed by modeling diffuse neutron scattering on $Na_2Ni_2TeO_6$ with reverse Monte Carlo method. The obtained results indicate two-dimensional nature of the magnetic correlations, and moreover, the symmetry of short-range magnetic state corresponds to long-range zigzag-type magnetic order in the honeycomb net, which was established earlier based on the theoretical calculations.

1. Introduction

Recently, increased interest of researchers for predicting, detecting and studying the unusual magnetic phenomena, in particular, searching for the new exotic magnetic structures

is observed. Much attention is paid to such objects as frustrated magnets,[1,2] Kagome lattices,[3,4] skyrmion lattices,[5,6] etc. From this point of view, low-dimensional systems are kind of fascinating interest, in which a quantum nature is evident on the level of the macroscopic collective phenomena such as quantum Hall effect,[7,8,9] giant magnetoresistance,[10,11] Berezinskii–Kosterlitz–Thouless topological phase transition (BKT),[12,13] existence of the ground states without long-range magnetic ordering (spin glasses, spin liquids[14,15]). Besides, two-dimensional materials are model systems for quantum fluctuations study associated with the high-temperature superconductivity.[16]

The systems, in which there are frustrations of different nature and anisotropy of the magnetic interactions, play herein an important role. A striking example of such objects is layered compounds with a honeycomb superstructure in the magnetic layers. Unlike triangular or Kagome lattices, where geometric frustrations take place, in these systems frustrations appear due to a competition between exchange interactions. On the honeycomb net, the difference between nearest and next-nearest interactions plays a crucial role. The corresponding J_1-J_2-J_3 quantum model was described in Ref. [17] and [18], where J_i correspond to exchange interactions between an atom and its i^{th} neighbor. Depending on the sign of J_1 and the sign and ratio of J_2/J_1 and J_3/J_1, different non-trivial spin configurations could be realized such as ‘zigzag’, ‘stripe’, different spiral structures, etc.[19]

The studied in the present work $Na_2Ni_2TeO_6$ compound is a representative of $A_2M_2TeO_6$ (A – alkali metal, M – transition metal) family, that is derived from a layered P2-type oxide with a hexagonal structure Na_xCoO_2-type. The initial studies of such compounds were motivated by their use as electrode material for alkali batteries. At the same time, due to the unique internal structure, the $A_2M_2TeO_6$ family is considered as a model system for low-dimensional magnetism. $Na_2Ni_2TeO_6$ compound is a layered oxide with a hexagonal layer structure, described in a framework of $P6_3/mcm$ space group.[20] In the structure, one can distinguish well-ordered magnetoactive layers with Ni and Te atoms isolated from each other

by non-magnetic Na-contained layers (**Figure 1**). The edge-sharing NiO_6 octahedra form a honeycomb lattice, where the TeO_6 octahedron is located in the center of each "comb". Due to such crystal structure, $Na_2Ni_2TeO_6$ could be attributed to a quasi-two-dimensional system, for which the magnetic interaction between adjacent Ni_2TeO_6 layers is much less than intralayer exchanges or non-existent.[18,19,21] It has to be noted, that the replacement of the composition in $A_2M_2TeO_6$ has a direct influence on its magnetic properties. So, the replacement of an alkali metal leads to a change of an interlayer distance, and as a result, it affects the interlayer magnetic interaction. In addition, the type and spin state of a transition metal atom play a crucial role.

Macromagnetic measurements showed the presence of a second-order phase transition at low temperatures in $Na_2Ni_2TeO_6$, associated with a transition from the paramagnetic to the magnetically ordered state.[21,22] There is a broad peak on the magnetic susceptibility curve near 27 K, related to the antiferromagnetic (AFM) phase transition. For classical antiferromagnets, a sharp maximum on the magnetic susceptibility curve at the Neel temperature T_N is usually observed. In our case, the broadened peak indicates the presence of the strong spin correlations above the phase transition and the overextending of magnetic order forming.[22] As an example, a resembling situation was previously observed for a number of compounds, in particular for $BaNi_2V_2O_8$, which also has a honeycomb arrangement of the magnetic layers.[23] Due to small interlayer interaction, $BaNi_2V_2O_8$ represents a good candidate for the 2D XY system. Neutron diffraction data also showed the strong two-dimensional correlations presence well above the T_N, which is primarily related to the BKT phase transition.

According to the neutron powder diffraction data from $Na_2Ni_2TeO_6$, the magnetic phase transition was observed at T_N = 27.5.[21] Signatures of both incommensurate and commensurate AFM spin ordering with propagation vector k = (1/2 0 0) were identified by the presence of different Bragg reflections on the neutron diffraction pattern. Based on the

first-principle density functional theory calculations, the most preferable magnetic ground state for the commensurate case is the FM zigzag chains AFM coupled. This result was obtained by consideration of three exchange interactions: FM between the nearest Ni atoms, AFM between the second neighbors (superexchange interaction Ni-O..O-Ni) and the weak AFM interaction between the layers. Magnetic zigzag-type ordering was previously observed for a number of other compounds with a honeycomb structure.[19,24,25,26] However, the long-order formation mechanisms in the low-dimensional systems remain unclear. A consequence of the Mermin – Wagner theorem is the absence of any spin ordering in 2D system at a temperature $T \neq 0$ K. However, any small interlayer exchange interaction or frustration in the magnetic structure break the theorem conditions, and therefore, can lead to the long-range magnetic order at a finite temperature $T > 0$. The spins of magnetic atoms begin to correlate with each other long before the phase transition, and the existence of still strong temperature fluctuations does not promote to the formation of long-range magnetic order.

In this paper, we report the study of the spin correlations related to the AFM phase transition in $Na_2Ni_2TeO_6$. Polarized neutron scattering experiment on a powder sample allowed us to detect and study magnetic diffuse scattering above the T_N. The magnetic lattice with correlated spins was modeled by reverse Monte Carlo method and the spin pair correlation function was reconstructed. In addition, the symmetry analysis of the short-range magnetic order in $Na_2Ni_2TeO_6$ was performed which was compared to zigzag-type long-range magnetic ordering.

2. Results and Discussion

The polarized neutron scattering experiment at the DNS instrument [27] was carried out in order to study the processes that occur with the magnetic lattice in $Na_2Ni_2TeO_6$. Measurements were carried out at the several temperatures T = 28 K, 29 K, 30 K, which are slightly higher than the phase transition temperature T_N. No visible difference between these

three temperatures was found therefore all the results will be presented only for the T = 30 K. The presence of additional diffuse neutron scattering in the magnetic channel within the small Q region was found (Figure 2). At this temperature, only the nuclear Bragg reflections corresponding crystal phase are observed on the neutron powder diffraction pattern, which indicates the long-range magnetic order absence in $Na_2Ni_2TeO_6$. On the other hand, the diffuse scattering points to disorder in the system that can be characterized by some kind of short-range ordering with a small correlation length. It is known that it can occur both from the crystal structure, for example, stacking faults in layered compounds or randomly ordered impurity, and from the spin structure. Since the diffraction process is can be considered as a Fourier transform, the short-range ordering leads to the broadened peaks on the neutron scattering pattern.

With XYZ polarization analysis, it was unequivocally established that the observed diffuse scattering has a magnetic nature. At least two features are observed near the $Q \approx 0.7$ Å^{-1} and $Q \approx 1.9$ Å^{-1}. The large measurement errors at $Q \approx 1.1$ Å^{-1} are associated with incorrect raw data conversion in the high-intensity nuclear peak region. The shape of the diffuse peaks is very important because it is determined by the spatial dimension of the scattering system. The theory of X-ray scattering on disordered graphite was developed by B. E. Warren,[28] who obtained expressions for the scattering intensity on a purely two-dimensional object represented by parallel and equidistant carbon layers but randomly ordered along the normal direction. It was shown that the diffraction pattern for the disordered 2D systems should contain diffuse peaks of the asymmetric shape described by the Warren function. Then, this model was adapted for the layered magnets with the short-range spin correlations in the layers and with the weak interaction between them.[29,30,31] In our case, the asymmetric shape of the peak is obvious, but this may be due to the presence of two close magnetic reflections at the small Q, which are the result of neutron scattering by the magnetic structure with the propagation vector k = (1/2 0 0) (Figure 2).

To define short-range magnetic correlations within a two-dimensional plane, the *Q*-dependence of magnetic diffuse scattering intensity was described by the Warren function. No additional parameters except the size of the correlation area were used for the approximation of the diffuse magnetic peak. The DNS data fitted with the Warren function at T = 30 K is shown in the Figure 3. The results indicate the two-dimensional nature of the magnetic correlations in $Na_2Ni_2TeO_6$ with characteristic correlation length $\xi \approx 15$ Å. Obviously, a corresponding coherent scattering area is insufficient for observing clear Bragg peaks, and we have a deal with the diffuse peaks on the neutron diffraction pattern.

For further analysis, the Spinvert program was used, which implements the reverse Monte Carlo (RMC) algorithm to fit a large network of spins to experimental powder diffraction data.[32] The main advantage of this approach is full independence of the spin Hamiltonian, the use of which is complicated for systems with the short-range spin correlations. This work is based on sequential experimental data fitting, where the neutron cross-section is calculated for a given spin configuration and compared with the experimental data at each step. However, Spinvert does not provide information about the ground magnetic state and spatial magnetic moments distribution in contrast to the ordinary Rietveld method for magnetic neutron powder diffraction. The RMC technique allows us to recover magnetic diffuse scattering pattern and the lattice averaged spin pair correlation function.

To generate the $Na_2Ni_2TeO_6$ input file for Spinvert, information about the crystal structure (lattice parameters and magnetic atoms positions) based on x-ray data full-profile analysis was used. The large 10x10x8 supercell with 6400 spins and periodic boundary conditions was chosen for the simulation. Then the RMC algorithm was applied with the realization of which the positions of magnetic moments are fixed to their crystallographic sites throughout the refinement, while their orientations are refined in order to satisfy the experimental data.

The resulting model curve for diffuse magnetic neutron scattering and experimental data are presented in Figure 4a. The corresponding spin configuration was used to reproduce the reciprocal space maps using complementary Spindiff program. The basic scattering planes (*hk*0), (*h*0*l*), and (0*kl*) are shown in Figure 4b – d. Thus, the smeared diffuse magnetic neutron scattering along the [00*l*] direction was found. First of all, this evidences about decreasing the correlations between adjacent honeycomb layers, hence, no 3D magnetic long-range ordering could be detected. Another important point is that these diffuse rods appear with a certain dependence. The maximum of neutron scattering is observed for $h = \pm (2n+1)/2$ within (*h*0*l*) plane and for $k = \pm (2n+1)$ within (0*kl*) plane for the integer *n*. This observation is correlated well with the previously obtained commensurate magnetic structure with propagation vector *k* = (1/2 0 0). It can be concluded that the translational symmetry is preserved during the phase transition from the short-range to the long-range magnetic ordering in $Na_2Ni_2TeO_6$. On the other hand, the symmetric diffuse scattering on the (*hk*0) plane indicates isotropy of spin correlations in this plane, that determined by the magnetic atoms honeycomb arrangement in the crystal structure. Thus, the reconstructed reciprocal space maps clearly indicate the two-dimensional picture of the spin correlations in $Na_2Ni_2TeO_6$ above T_N.

To understand the diffuse scattering nature in $Na_2Ni_2TeO_6$, the spin pair correlation function in real space ($\vec{\boldsymbol{S}}(0) \cdot \vec{\boldsymbol{S}}(r)$) was reconstructed. Each point in Figure 5 corresponds to a certain distance between the neighboring spins. The corresponding magnetic moments are parallel to each other in the case of a positive spin pair correlation function value and antiparallel in the opposite case. The nearest neighbors of Ni atoms located at a distance of ≈ 3 Å, and according to the data, their spins should be strongly coupled and pointed into the same direction. On the other hand, for the second and the third neighbors in the honeycomb structure, a predominant AFM interaction is obtained, which leads to a negative sign of the spin pair correlation function. Based on this, it can be concluded that the obtained result is in complete accordance with the assumed commensurate zigzag-type magnetic order below the

T_N (inset in Figure 5). Thus, during the phase transition, not only the translational symmetry but also the magnetic lattice symmetry with respect to the spin reversal operator is preserved. It should be noted that the spin correlations function damp sharply with increasing distance and almost fade out at $r \approx 15$ Å which is consistent with the results of Warren function approximation.

3. Conclusion

In this work, an experimental study of the long-range magnetic order formation in a quasi-two-dimensional system with honeycomb geometry represented by $Na_2Ni_2TeO_6$ was performed. Particularly, it was found that the previously observed features on the magnetic susceptibility curve are associated with the presence of strong spin correlations above the T_N. As a result, an overextended phase transition from the paramagnetic to a magnetically ordered phase occurs in the system, which, at the first stage, manifests itself in the gradual formation of a structure with short-range magnetic order. Our results indicate the translational and magnetic symmetry of the state with strong magnetic correlations above the T_N corresponds to the previously published zigzag-type long-range magnetic order. An evidence of this behavior is the presence of diffuse magnetic scattering, from which we have extracted important information about the two-dimensional nature of spin correlations in the $Na_2Ni_2TeO_6$.

4. Experimental Section

A polycrystalline sample of $Na_2Ni_2TeO_6$ was synthesized by solid-state reactions, as previously described in Ref. [20]. The sample is well crystallized: a single phase, a stoichiometry and a crystal structure were refined by X-ray analysis. The low-temperature polarized neutron diffraction was carried out on the Diffuse Neutron Scattering spectrometer DNS at the MLZ research center (Garching, Germany).[27] The main assignment of the

instrument is to distinguish different contributions to the total neutron scattering cross section such as nuclear coherent, nuclear incoherent and magnetic scattering, with a polarized neutron beam. Monochromatic neutrons with wavelength λ = 4.2 Å were used. The polarization was controlled by Helmholtz ring system, which allows to create a magnetic field at the sample and to change its direction and magnitude as well. The field strength is large enough to ensure the adiabatic rotation of the neutron spin orientation but small enough to affect the sample magnetization. Spin-flip and non-spin-flip neutron scattering cross sections were measured for incident beam polarization along three main directions *x*, *y*, and *z*. The orthogonal coordinate system is the following: *x* is parallel to the scattering vector *Q*; *y* and *z* are perpendicular to *Q* pointing in- and out-of-the scattering plane respectively. Thus, during the measurements, six different data sets are obtained for the neutron scattering intensity dependencies as functions of *Q*. The subsequent XYZ polarization analysis[33] based on the Maleev-Blume theory[34,35] was performed to separate the magnetic, nuclear incoherent and nuclear coherent contribution to the total neutron scattering cross section. DNS data analysis was performed using the reverse Monte Carlo method, which is implemented in the Spinvert program.[32]

Acknowledgements

The authors are grateful to V.B. Nalbandyan for providing the sample, to K.S. Nemkovsky for discussing the details of the experiment, and T. Müller for his help in conducting the experiment. The authors thank for support Russian Foundation for Basic Research (grant # 18-32-00226).

Received: ((will be filled in by the editorial staff))
Revised: ((will be filled in by the editorial staff))
Published online: ((will be filled in by the editorial staff))

References

[1] A. P. Ramirez, *Annu. Rev. Mater. Sci.* **1994,** *24*, 453.

[2] O. A. Starykh, *Rep. on Prog. in Phys.* **2015**, *78*, 052502.

[3] J. S. Helton, K. Matan, M. P. Shores, E. A. Nytko, B. M. Bartlett, Y. Yoshida, Y. Takano, A. Suslov, Y. Qiu, J. -H. Chung, D. G. Nocera, Y. S. Lee, *Phys. Rev. Lett.* **2007**, *98*, 107204.

[4] R. Chisnell, J. S. Helton, D. E. Freedman, D. K. Singh, R. I. Bewley, D. G. Nocera, Y. S. Lee, *Phys. Rev. Lett.* **2015**, *115*, 147201.

[5] S. Mühlbauer, B. Binz, F. Jonietz, C. Pfleiderer, A. Rosch, A. Neubauer, R. Georgii, P. Böni, *Science* **2009**, *323*, 915.

[6] X. Z. Yu, Y. Onose, N. Kanazawa, J. H. Park, J. H. Han, Y. Matsui, N. Nagaosa, Y. Tokura, *Nature* **2010**, *465*, 901.

[7] K. von Klitzing, G. Dorda, M. Pepper, *Phys. Rev. Lett.* **1980**, *45*, 494.

[8] D. C. Tsui, H. L. Stormer, A. C. Gossard, *Phys. Rev. Lett.* **1982**, *48*, 1559.

[9] Y. Zhang, Y. -W. Tan, H. L. Stormer, P. Kim, *Nature* **2005**, *438*, 201.

[10] G. Binasch, P. Grünberg, F. Saurenbach, W. Zinn, *Phys. Rev. B* **1989**, *39*, 4828.

[11] M. N. Baibich, J. M. Broto, A. Fert, F. Nguyen Van Dau, F. Petroff, *Phys. Rev. Lett.* **1988**, *61*, 2472.

[12] V. L. Berezinskii, *Sov. Phys. JETP* **1971**, *32*, 493.

[13] J. M. Kosterlitz, D. J. Thouless, *J. Phys. C* **1973**, *6*, 1184.

[14] S. T. Bramwell, M. J. P. Gingras, *Science* **2001**, *294*, 1495.

[15] L. Balents, *Nature* **2010**, *464*, 199.

[16] E. Manousakis, *Rev. Mod. Phys.* **1991**, *63*, 1.

[17] J. B. Fouet, P. Sindzingre, C. Lhuillier, *Eur. Phys. J. B* **2001**, *20*, 241.

[18] P. H. Y. Li, R. F. Bishop, D. J. J. Farnell, C. E. Campbell, *Phys. Rev. B* **2012**, *86*, 144404.

[19] E. A. Zvereva, M. I. Stratan, Y. A. Ovchenkov, V. B. Nalbandyan, J. -Y. Lin, E. L. Vavilova, M. F. Iakovleva, M. Abdel-Hafiez, A. V. Silhanek, X. -J. Chen, A. Stroppa, S. Picozzi, H. O. Jeschke, R. Valentí, A. N. Vasiliev, *Phys. Rev. B* **2015**, *92*, 144401.

[20] M. A. Evstigneeva, V. B. Nalbandyan, A. A. Petrenko, B. S. Medvedev, A. A. Kataev, *Chem. Mater.* **2011**, *23*, 1174.

[21] S. K. Karna, Y. Zhao, R. Sankar, M. Avdeev, P. C. Tseng, C. W. Wang, G. J. Shu, K. Matan, G. Y. Guo, F. C. Chou, *Phys. Rev. B* **2017**, *95*, 104408.

[22] R. Sankar, I. Panneer Muthuselvam, G. J. Shu, W. T. Chen, S. K. Karna, R. Jayavel, F. C. Chou, *CrystEngComm* **2014**, *16*, 10791.

[23] N. Rogado, Q. Huang, J. W. Lynn, A. P. Ramirez, D. Huse, R. J. Cava, *Phys. Rev. B* **2002**, *65*, 144443.

[24] A. I. Kurbakov, A. N. Korshunov, S. Y. Podchezertsev, A. L. Malyshev, M. A. Evstigneeva, F. Damay, J. Park, C. Koo, R. Klingeler, E. A. Zvereva, V. B. Nalbandyan, *Phys. Rev. B* **2017**, *96*, 024417.

[25] E. Lefrançois, M. Songvilay, J. Robert, G. Nataf, E. Jordan, L. Chaix, C. V. Colin, P. Lejay, A. Hadj-Azzem, R. Ballou, V. Simonet, *Phys. Rev. B* **2016**, *94*, 214416.

[26] C. Wong, M. Avdeev, C. D. Ling, *Journal of Solid State Chemistry* **2016**, *243*, 18.

[27] Y. Su, K. Nemkovskiy, S. Demirdis, *Journal of large-scale research facilities* **2015**, *1*, 27.

[28] B. E. Warren, *Phys. Rev.* **1941**, *59*, 693.

[29] C. S. Knee, D. J. Price, M. R. Lees, M. T. Weller, *Phys. Rev. B* **2003**, *68*, 174407.

[30] L. Clark, G. Sala, D. D. Maharaj, M. B. Stone, K. S. Knight, M. T. F. Telling, X. Wang, X. Xu, J. Kim, Y. Li, S. W. Cheong, B. D. Gaulin, *Nature Physics* **2019**, *15*, 262.

[31] S. M. Yusuf, J. M. Teresa, P. A. Algarabel, M. D. Mukadam, I. Mirebeau, J.-M. Mignot, C. Marquina, M. R. Ibarra1, *Phys. Rev. B* **2006**, *74*, 184409.

[32] J. A. M. Paddison, J. R. Stewart, A. L. Goodwin, *J. Phys. Condens. Matter* **2013**, *25*, 454220.

[33] W. Schweika, *J. Phys. Conf. Ser.* **2010**, *211*, 012026.

[34] S. V. Maleev, V. G. Bar'yaktar, R. A. Suris, *Sov. Phys. Solid State* **1963**, *4*, 2533.

[35] M. Blume, *Phys. Rev.* **1963**, *130*, 1670.

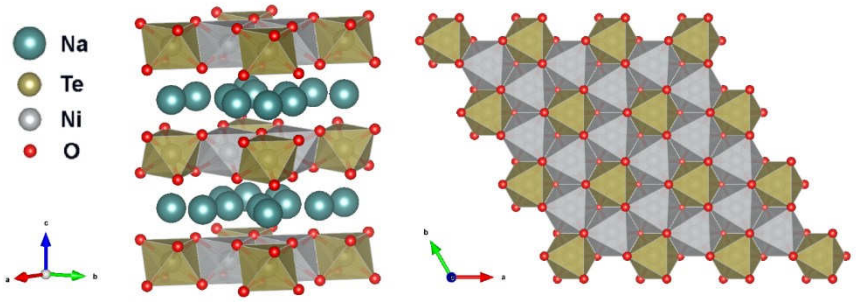

Figure 1. Left: General view of the crystal structure of $Na_2Ni_2TeO_6$. Right: 2D honeycomb lattice of NiO_6 octahedra (in the center of each "comb" is located the TeO_6 octahedron).

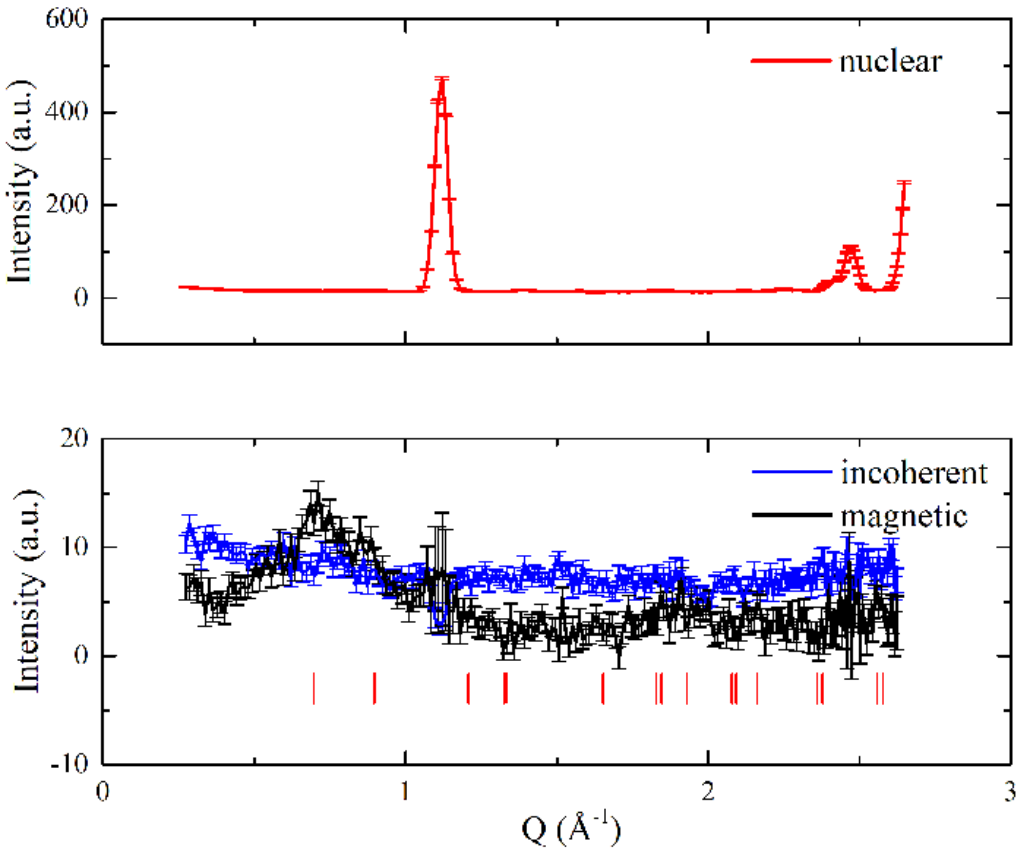

Figure 2. Separation of nuclear coherent (upper panel), magnetic coherent (black curve, lower panel) and nuclear incoherent scattering (blue curve, lower panel) by XYZ polarization analysis on the DNS. The vertical ticks show the positions of the magnetic Bragg reflections associated with the propagation vector k = (1/2 0 0).

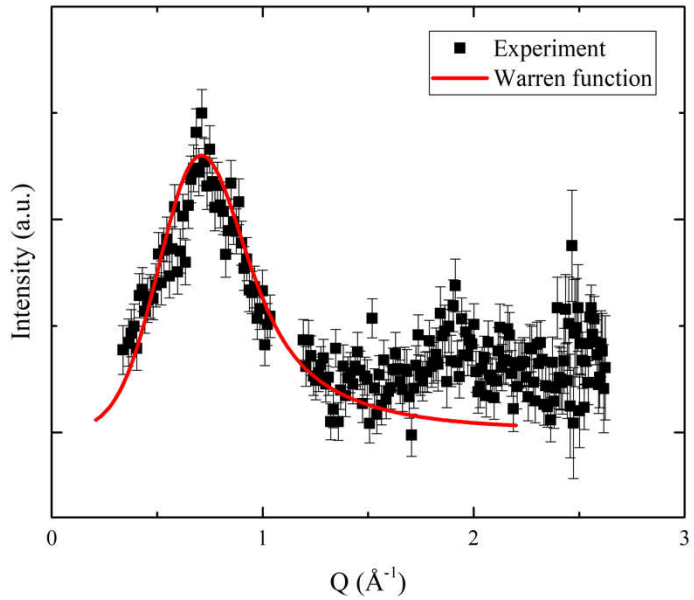

Figure 3. Experimentally measured diffuse magnetic neutron scattering (black dots with error bars) and the fit of the Warren function to the data (red solid line).

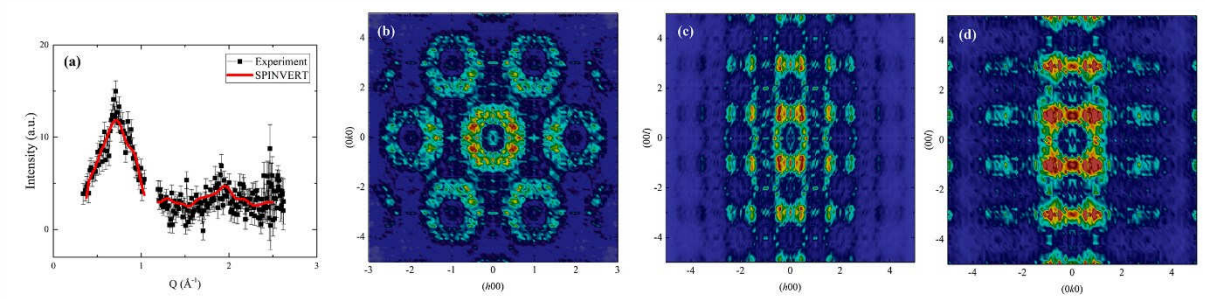

Figure 4. a) Experimentally measured diffuse magnetic neutron scattering (black dots with error bars) and the theoretically calculated curve obtained by the reverse Monte Carlo method (red solid line). b-d) Reconstructed magnetic neutron scattering maps for the (*hk*0), (*h*0*l*) and (0*kl*) planes in reciprocal space.

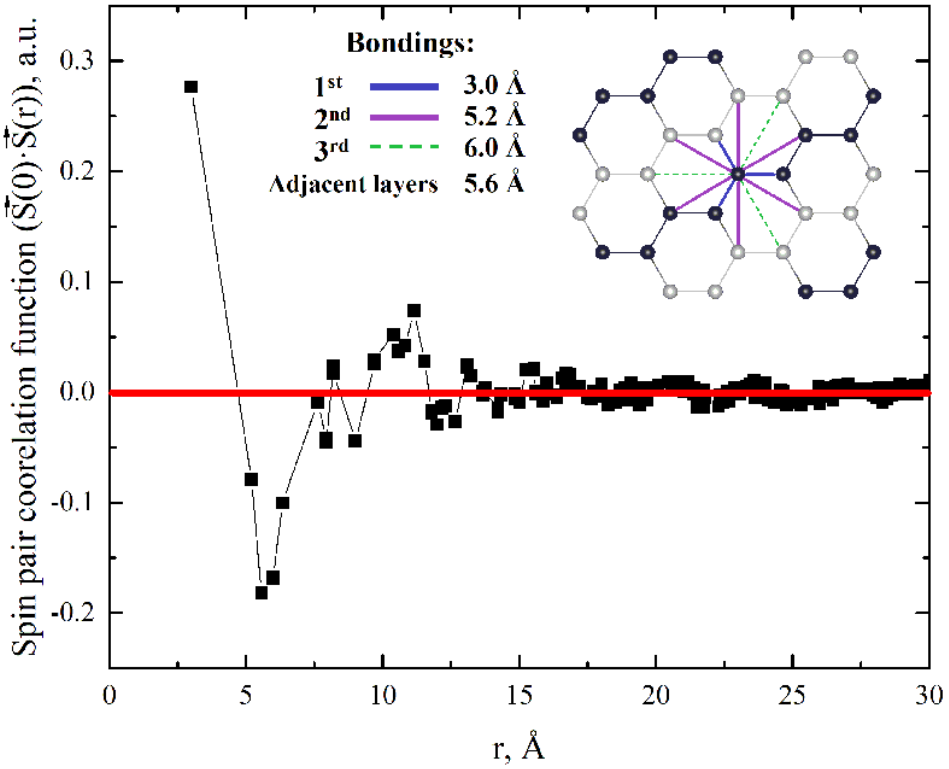

Figure 5. The reconstructed spin pair correlation function. Inset: a schematic view of a zigzag-type magnetic structure (different colors of the circles correspond to opposite directions of the spins); different lines indicate the bonds of Ni atom with neighbors in different coordination spheres. The table presents the bond lengths with neighboring Ni atoms in the honeycomb layer and the distance between adjacent layers (not specified in the figure).